Intersection and anticrossing of far-infrared modes in elliptical quantum dots with tunable ellipticity

M. Hochgräfe, Ch. Heyn, and D. Heitmann
Institut für Angewandte Physik und Zentrum für Mikrostrukturforschung, Universität Hamburg, Jungiusstraße 11, D-20355 Hamburg, Germany

(Received 27 June 2000; revised manuscript received 4 October 2000; published 22 December 2000)

We have investigated elliptically shaped quantum dots in modulation-doped $Al_xGa_{1-x}As$-GaAs heterostructures with far-infrared spectroscopy. We observe series of modes ω_{+i} and ω_{-i} which increase in frequency with increasing mode index *i*. The frequencies ω_{+i} and ω_{-i} at a given *i* represent, at a magnetic field $B=0$, oscillations along the short and long axes of the dot, respectively. With a gate voltage we can vary the ellipticity of the dot; in particular, we can tune the ω_{-2} mode through the ω_{+1} mode. This leads to an interesting mode intersection and, at $B>0$, to an anticrossing behavior.

DOI: 10.1103/PhysRevB.63.035303 PACS number(s): 73.20.Mf, 78.30.Fs, 71.10.−w

With sophisticated lithography and etching techniques it is possible to fabricate quantum dots of arbitrary shape, starting from modulation-doped $Ga_{0.67}Al_{0.33}As$-GaAs heterostructures. The excitation spectrum of such quantum dots can be investigated most conveniently with far-infrared (FIR) spectroscopy. The simplest situation is a circular shaped dot with parabolic confinement $V(x,y)=\frac{1}{2}m^*\omega_0^2(x^2+y^2)$, where *x* and *y* are the coordinates in the plane of the original two-dimensional electron system (2DES). Then, according to the generalized Kohn theorem,[1] one observes, at magnetic field $B=0$, *one* mode at the frequency ω_0 of the *external* or *bare* potential. With increasing *B* the mode splits into two, one with a positive dispersion (ω_{+1}) and one with a negative dispersion (ω_{-1}). For circular shaped dots with a nonparabolic confinement potential, one observes additional sets of high-frequency modes $\omega_{\pm i}$, with $i=1,2,3,...$, which split again with $B>0$ into two branches with positive- and negative-*B* dispersions. These modes can be described in a localized plasmon model (see, for example Refs. 2 and 3, and our discussion below). An interesting point is that in the latter case modes ω_{+i} intersect with modes $\omega_{-j}(j>i)$ in a magnetic field. As shown theoretically and experimentally, a non-circular-shaped dot is required to lift the degeneracy of the intersecting modes, leading to an anticrossing behavior, whichs strength is strongly governed by electron-electron-interaction effects.[4,5] In our paper we are interested in elliptically shaped dots. If the external potential is parabolic along the short (*x*) axis and the long (*y*) axis, $V(x,y)=\frac{1}{2}m^*(\omega_x^2x^2+\omega_y^2y^2)$, one expects, according to the generalized Kohn theorem, two modes ω_{+1} and ω_{-1} in a magnetic field *B*, which have, in contrast to circular dots, different frequencies at $B=0$.[6,7] The corresponding FIR excitations are center-of-mass oscillations along the short and long axes, respectively. We have prepared quantum dots of elliptical shape with nonparabolic potentials which can be tuned with a gate voltage V_G. We observe a rich mode spectrum with *several* sets of modes ω_{+i} and ω_{-i}, $i=1,2,3,...$. A unique situation in our elliptically shaped dots is that we can increase the mode splitting at $B=0$, $\Delta\omega_i=\omega_{+i}-\omega_{-i}$, so strongly that the frequency ω_{-2} decreases below the ω_{+1} mode so, in contrast to circular or quadratic dots, the experimental sequence of the observed modes has not alternating negative and positive *B* dispersions. Here the interesting question arises of whether or not mode repelling occurs in such a situation.

Arrays of elliptical quantum dots have been prepared starting from 2DES in modulation-doped $Ga_{0.67}Al_{0.33}As$-GaAs heterostructures with an additional Si-δ-doped backgate 200 nm underneath the 2DES. The electron density and the mobility were $N_S=3.14\times10^{11}\,cm^{-2}$ and $\mu=620\,000\,cm^2/V\,s$ respectively. A photoresist grid mask was prepared by a holographic double exposure with an in-between 90° rotation as in Refs. 5 and 8. The period $a=600\,nm$, was the same in both directions, but the exposure in the *x* direction was longer than in the *y* direction. Then a dry-etching process with nominal 180-nm etching depth was performed. A Ti gate of 10 nm was evaporated onto the structure. After the evaporation we obtain samples as shown in Fig. 1. The geometrical shape of our structure here is actually very similar to samples prepared in Ref. 9. The samples in Ref. 9 had wider geometrical wires and a higher electron density, and form quantum wires with a modulated density. Here we find that

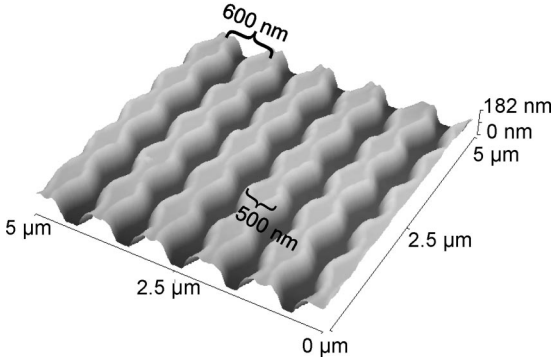

FIG. 1. AFM image of sample A after dry etching and evaporating of the Ti gate. In the narrow regimes of the lithographically defined wires, the electrons are completely depleted. Elliptical dots are formed. The lithographic width of the wire, at maximum, is $w_x=500\,nm$.

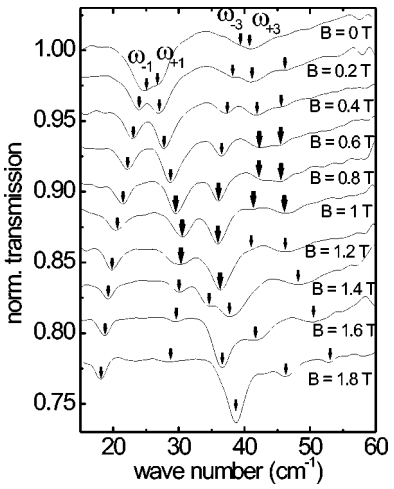

FIG. 2. Spectra of sample A at $V_G = 0.8$ V corresponding to $N = 320$ from $B = 0$ T to $B = 1.8$ T incremented by 0.2 T. Spectra are shifted vertically for $B > 0$ for clarity. The resonance positions are marked by arrows. The regime where an anticrossing of the modes occurs is marked by thick arrows. Fits to the dispersion (Fig. 4) let us identify the modes as $\omega_{\pm 1}$ and $\omega_{\pm 3}$.

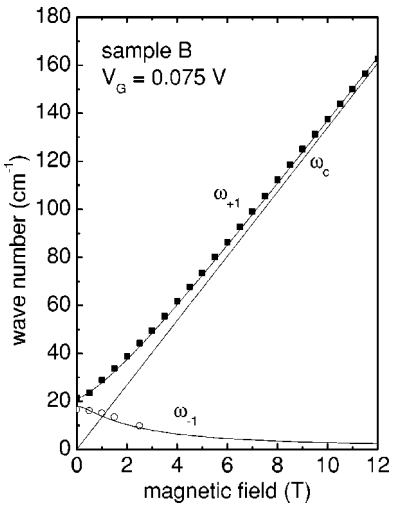

FIG. 3. Dispersion of sample B at $V_G = 0.075$ V corresponding to eight electrons per dot. Full lines are fits using Eq. (1) with $\omega_x = 21.5\,\mathrm{cm}^{-1}$ and $\omega_y = 18\,\mathrm{cm}^{-1}$. The dashed line is the cyclotron resonance of the 2DES which is suppressed in dots. Here and in the following figures modes are marked by full (empty) symbols, if the excitation is polarized along the short (long) axis of the quantum dot at $B = 0$.

due to the smaller width and the gate, the electron system is depleted in the narrow regime, so that actually isolated elliptical dots are formed. The electron density N_S and the shape of the potential could be changed through a voltage V_G between the gate and the Si-δ-doped backgate. Here in particular we discuss two different samples A and B with different electron numbers at $V_G = 0$. FIR transmission experiments in a perpendicular magnetic field have been performed in a superconducting magnet, which was connected to a Fourier transform spectrometer. The spectral resolution was set to $0.5\ \mathrm{cm}^{-1}$ and the temperature was 1.8 K. In the following we plot the relative transmission $T(V_G)/T(V_{\mathrm{Th}})$, where V_{Th} is the threshold voltage where the electron system is completely depleted.

As an example for experimental spectra, in Fig. 2 we show measurements for sample A at $V_G = 0.8$ V ($V_{\mathrm{Th}} = -0.2$ V). At $B = 0$ there are two sets of closely separated resonances. These resonances separate increasingly in a magnetic field and eventually undergo several anticrossings. At high magnetic fields ($B = 9$ T) nearly all the oscillator strength is concentrated in one cyclotronlike mode. This allows us to extract from the integrated intensity the averaged electron density $\tilde{N}_S$ and then, from the known unit cell a^2, the number of electrons per dot $N = \tilde{N}_S a^2$.[10] For sample A at $V_G = 0.8$ V the values are $\tilde{N}_S = 8.92 \times 10^{10}\,\mathrm{cm}^{-2}$ and $N = 320$. We have also performed experiments with linearly polarized radiation. At small B this allows us to evaluate the direction of the excited charge oscillations. In the following we discuss the dispersion derived from such experimental spectra. Modes which have a linear polarization along the short (long) axis at small B are marked by full (open) symbols.

In Fig. 3 we show the experimental dispersion of sample B at $V_G = 0.075$ V ($V_{\mathrm{Th}} = -0.1$ V) corresponding to $N = 8$ electrons per dot. We observe two branches which, in contrast to circular or quadratic shaped dots,[5] are split into two resonances at $B = 0$. These two resonances correspond to oscillations along the long and short axes of the ellipse, which can be extracted directly from the corresponding polarization behavior. The low-frequency branch decreases in intensity with increasing B and can, due to the decreasing sensibility of our experimental setup at low frequencies, no longer be resolved at larger B. The high-frequency branch increases in intensity with increasing B, similar to what is known for circular dots. It approaches the cyclotron resonance frequency ω_C. The cyclotron resonance itself is not observed in the experiment as expected for isolated dots.

This experimental dispersion can be perfectly described by transitions between single-particle energies of the external potential,[6,7]

$$\omega_{\pm}^2 = \tfrac{1}{2}\left[\omega_x^2 + \omega_y^2 + \omega_C^2 \pm \sqrt{\omega_C^4 + 2\omega_C^2(\omega_x^2 + \omega_y^2) + (\omega_x^2 - \omega_y^2)^2}\right], \tag{1}$$

where $\omega_C = eB/m^*$ is the cyclotron resonance frequency, and m^* is the effective mass. This indicates that for sample B at $V_G = 0.075$ V the external potential is nearly parabolic both in x and y directions. Then, according to the general Kohn theorem,[1] the dipole excitation of the many-body electron system is a rigid center-of-mass oscillation which occurs exactly at the transition frequency of the single-particle spectrum of the external potential, independently of how many electrons are in the dots. This two-mode behavior was observed in several diploma and Ph.D. theses (see, e.g., Refs. 11 and 12), but to our knowledge has not been published in a journal.

In Fig. 4 we show measurements of sample A at different V_G. Here we observe not only the two fundamental Kohn modes, but sets of modes which undergo different types of

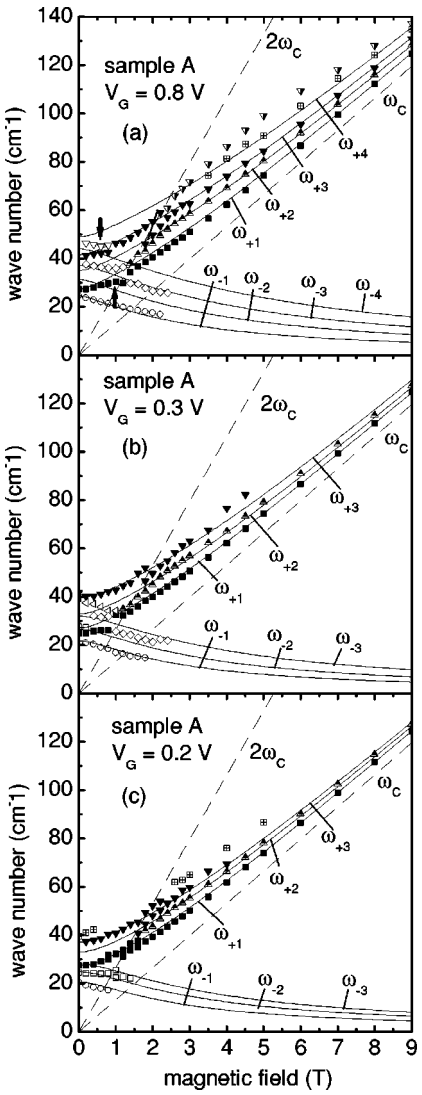

FIG. 4. Experimental dispersions of sample A at (a) $V_G = 0.8\,\mathrm{V}$, (b) $V_G = 0.3\,\mathrm{V}$, and (c) $V_G = 0.2\,\mathrm{V}$, with corresponding electron numbers per dot of $N = 320$, 140, and 90, respectively. The arrows mark the anticrossing of the modes.

anticrossings in a magnetic field. This directly indicates that the external potential is no longer parabolic. To describe this behavior we expand the edge-magnetoplasmon model of Fetter.[2] In a finite-sized 2DES of radius R, for $B=0$ one obtains the energies of the magnetoplasmon as[2]

$$\omega_{\pm i}^2 = f_1 \frac{Ne^2}{2m^*\epsilon_0\epsilon^*\pi}\,\frac{i}{R^3} = f_i\omega_0^2 i, \quad i = 1,2,3,\ldots. \qquad (2)$$

ϵ^* is the effective dielectric constant, and f_1 is a constant which depends slightly on the shape of the potential and its value is $f_1 = 1(0.81)$ in the model of[2].[13] In these models the modes are 2D plasmon modes which are ''confined,'' with a different number of nodes, in the finite-sized dots. For an elliptically shaped dot we expect, by replacing ω_0 in Eq. (2) by ω_x and ω_y in the respective direction,

$$\omega_{\pm i}^2 = \frac{1}{2}\left[\omega_{xi}^2 + \omega_{yi}^2 + \omega_C^2 \pm \sqrt{\omega_C^4 + 2\omega_C^2(\omega_{xi}^2 + \omega_{yi}^2) + (\omega_{xi}^2 - \omega_{yi}^2)^2}\right], \qquad (3)$$

with $\omega_{xi}^2 = f_i\omega_x^2 i$ and $\omega_{yi}^2 = f_i\omega_y^2 i$. Within this approximation we assume that f_i is the same in the x direction as well as the y direction. Indeed, except for the anticrossing, the experimental dispersions in Fig. 4 are quite well described by this expression. This suggests that the higher-frequency modes $i = 2,3,\ldots$ correspond to higher confined plasmon modes.

Note that some modes, in particular the ω_{+2} mode, have a very low oscillator strength at small B, and can only be observed above the regime of the Bernstein modes which are explained below. We believe that this arises from the symmetry of these even number modes.

From Figs. 4(a)–4(c), we observe that there are actually two different types of anticrossings in the dispersions. One type occurs close to $2\omega_C$, and resembles the interaction of plasmons in a 2DES with the Bernstein modes. Similar interactions were also observed in nonparabolic circular dots, and discussed extensively in Ref. 14. We will not elaborate on this here. Another type of anticrossing occurs if a higher-order ω_{-i} mode intersects with an ω_{+j} mode ($i > j$). Model calculations for few-electron systems[4] have shown that such an anticrossing does not occur for circularly shaped dots, even if the potential is not parabolic; rather, it was shown that a noncircular, shape of the dot, for example a quadratic shape, is required to break the symmetry. It was discussed in Ref. 9 that, besides the symmetry and geometry, the electron-electron interaction determines the strength of the interaction and the resulting splitting in the anticrossing regime. We believe that the same parameters, the geometrical shape and the electron-electron interaction, are responsible for the anticrossing at $B > 0$ that we observe for our elliptically shaped dots. A very interesting behavior occurs if we go to low gate voltages, e.g., $V_G = 0.2\,\mathrm{V}$ in Fig. 4(c), because then the two lowest modes both show a negative-B dispersion. Such a situation is not possible for circular or quadratic dots. Obviously we have increased the ellipticity of the dots with decreasing gate voltage so strongly that the frequency of the ω_{-2} mode becomes smaller than the ω_{+1} mode.

The assignment of these modes can be confirmed by linear polarization experiments. Linearly polarized measurements are not easy to perform in our cryogenic environment, which requires wave-guide optics. Although we could not expect perfect polarizations in both directions we can clearly distinguish each mode. Figure 5 shows spectra at $V_G = 0.2\,\mathrm{V}$ for $B = 0 - 0.6\,\mathrm{T}$ in the directions parallel to the long axis (y-polarized direction) and parallel to the short axis (x-polarized direction) of the elliptical dots. If we compare the signal strengths of the two modes with the lowest energies in both directions, the result is that in the y-polarized direction the modes are significantly stronger than in the x direction. Therefore, these modes have the same linear polarization. In contrast, the ω_{+1} mode has a larger oscillator strength in the x-polarized direction.

In the following we would like to discuss several aspects of the dispersions, and in particular its gate voltage depen-

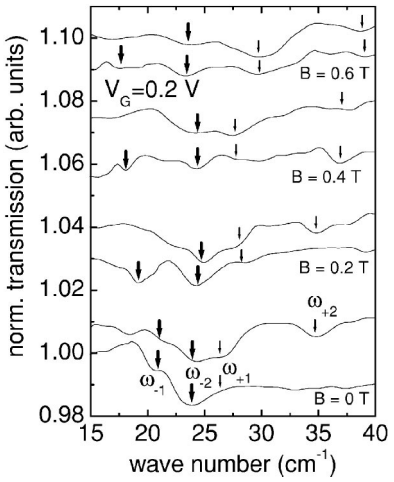

FIG. 5. Experimental spectra of sample A at $V_G = 0.2$ V for low magnetic fields B for linear polarized radiation. Spectra are shifted vertically for clarity. The dashed lines are spectra with radiation parallel to the long axis, and the full lines are spectra parallel to the short axis of the elliptical dot. The y- (x-) polarized modes are marked by thick (thin) arrows.

dence in more detail. For this in Fig. 6(a) have plotted the experimental resonance positions $\omega_{\pm i}$ at $B=0$, in Fig. 6(b) the splitting $\Delta_i = \omega_{+i} - \omega_{-i}$, and in Fig. 6(c) the extracted potential parameter f_i/f_1 and electron number N. In Fig. 6(a) we see that in the regime $V_G = 1.2-0.4$ V the fundamental modes ω_{+1} and ω_{-1} stay nearly constant. This is consistent with the expectation from Kohns' theorem that, if the shape of the external potential stays the same while varying V_G, the frequency does not depend on N. Higher index modes are not restricted by Kohns' theorem. They indeed show a slight decrease of the $B=0$ resonance frequency. This is also reflected in the ratio f_i/f_1. What is surprising is that these ratios are smaller than 1. For a strict hard wall potential, the Fetter model, one would expect 1. In experiments in etched quantum dots usually f_i/f_1 is even larger than 1 (see, for example, Ref. 5). We have no definite explanation for this. We believe that our complex geometry with the gate also on the sidewalls of the etched structures creates such an unusual potential. If we decrease the gate voltage below 0.4 V, in Fig. 6(a) we observe a very sudden drop of the ω_{-i} modes, in such a way that they decrease below the respective ω_{+i} modes which stay nearly constant, and lead to the unusual situation mentioned above that two modes with negative B dispersion lay below the ω_{+1} mode.

At the same time, the corresponding gaps in Fig. 6(b) increase drastically. It is not clear to us whether this behavior arises purely from a sudden change of the external potential, in particular in the long axis direction of the elliptically shaped dot. That the external potential does not follow the gate voltage in an absolutely smooth way can also be inferred from the fact that the electron number N in Fig. 6(c) exhibits a small bump in its dependence on V_G in this regime. For the anticrossings at $B>0$, we have seen above that the dispersion is significantly influenced by mode repelling enhanced by electron-electron interaction.[4] In a certain sense

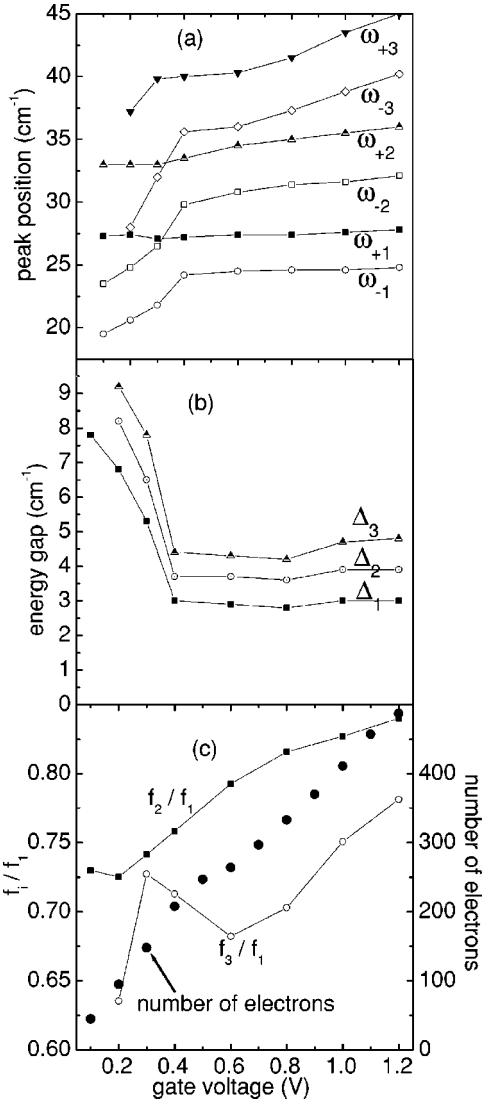

FIG. 6. Peak positions at $B=0$ (a), energy gaps $\Delta_i = \omega_{+i} - \omega_{-i}$ at $B=0$ (b), extracted potential parameter f_i/f_1 and electron number N (right axis) (c) vs the gate voltage V_G for sample A.

we can visualize the situation that ω_{-2} decreases below ω_{+1} by shifting the anticrossing from finite B to $B=0$. In such a model we would indeed expect that not only the external potential, but also mode repelling, would determine the dispersion and the gap. However, whereas for $B>0$ an ω_{+i} mode can interact with an ω_{-j} mode, for $B=0$ we expect that the $\omega_{-i}(\omega_{+i})$ modes can only interact with $\omega_{-j}(\omega_{+j})$ modes, since at $B=0$ ''+'' and ''−'' modes oscillate either along the long or the short axis and are thus decoupled. Note that for the special situation $\omega_{-2}(B=0) = \omega_{+1}(B=0)$, not only the dynamic excitations, but also the underlying energy spectrum, exhibit a degeneracy, a degeneracy produced artificially by tuning the system. These discussions show that in tunable elliptical dots rich scenarios of mode coupling, repelling, and anticrossings can occur. However, full self-consistent calculations are highly desirable to make definite statements.

In summary, we have prepared elliptically shaped quan-

tum dots with a tunable ellipticity. These dots show a rich mode spectrum and a variety of anticrossings and mode intersections that goes far beyond that of circular or quadratic dots studied so far.

We gratefully acknowledge financial support by the ''Deutsche Forschungsgemeinschaft'' through SFB 508 ''Quantum Materials'' and the Graduiertenkolleg ''Nanostrukturierte Festkörper.''

[1] P. Maksym and T. Chakraborty, Phys. Rev. Lett. **65**, 108 (1990).
[2] A. L. Fetter, Phys. Rev. B **32**, 7676 (1985); **33**, 3717 (1986).
[3] V. Shikin, S. Nazin, D. Heitmann, and T. Demel, Phys. Rev. B **43**, 11 903 (1991).
[4] D. Pfannkuche and R. Gerhardts, Phys. Rev. B **44**, 13 132 (1991).
[5] T. Demel, D. Heitmann, P. Grambow, and K. Ploog, Phys. Rev. Lett. **64**, 788 (1990).
[6] S. K. Yip, Phys. Rev. B **43**, 1707 (1991).
[7] Q. P. Li, K. Karrai, S. K. Yip, S. Das Sarma, and H. D. Drew, Phys. Rev. B **43**, 5151 (1991).
[8] K. Bollweg, T. Kurth, D. Heitmann, V. Gudmundsson, E. Vasiliadou, P. Grambow, and K. Eberl, Phys. Rev. Lett. **76**, 2774 (1996).
[9] M. Hochgräfe, Ch. Heyn, and D. Heitmann, Phys. Rev. B **60**, R13974 (1999).
[10] U. Merkt, in *Advances in Solid State Physics*, edited by U. Rössler (Vieweg, Braunschweig, 1990), Vol. 30, p. 77.
[11] K. Kern, Ph.D. thesis, Stuttgart, 1991.
[12] T. Kurth, Ph.D. thesis, Hamburg, 1997.
[13] V. B. Sandormirski, V. A. Volkov, G. R. Aizin, and S. A. Mikhailov, Electrochim. Acta **34**, 3 (1989).
[14] V. Gudmundsson, A. Brataas, P. Grambow, B. Meurer, T. Kurth, and D. Heitmann, Phys. Rev. B **51**, 17 744 (1995).